

Unified description and validation of Monte Carlo simulators in PET

Irène Buvat¹, Isabella Castiglioni², Juliette Feuardent¹
and Maria-Carla Gilardi²

¹ U494 INSERM, CHU Pitié-Salpêtrière, Paris, France

² INB—CNR, Università di Milano—Bicocca, Istituto H S Raffaele, Milano, Italy

E-mail: buvat@imed.jussieu.fr

Received 5 August 2004, in final form 21 November 2004

Published 5 January 2005

Online at stacks.iop.org/PMB/50/329

Abstract

Several Monte Carlo simulators are currently available for positron emission tomography (PET). Because each code has been described in a different way, it is difficult to know which one is best suited to a specific application. To help clarify the capabilities and accuracy of different codes dedicated to PET simulations, we propose a uniform description of the code features. This description specifies features pertaining to the models used for simulating the physics of PET and for describing a PET acquisition, to the acceleration strategies and to the technical characteristics of the code implementation. To assess the code accuracy, we suggest validation procedures based on NEMA phantoms involving standard physical parameters and simulation of a complex activity distribution. A test characterizing the statistical properties of detected coincidences is also described. The proposed code description and validation procedures are illustrated by considering the SimSET and PET-EGS codes. These codes differ in many features, including models for randoms and dead time, and source description. Despite these differences, both codes yielded data with properties close to those of real data. Depending on the intended application, one code might be preferred however. Indeed, only PET-EGS allows for accurate modelling of count rates while SimSET is more computationally efficient. The proposed code description and validation procedures might help determine which code is most appropriate for a specific application.

1. Introduction

Monte Carlo simulations are currently widely used in positron emission tomography (PET) imaging for optimizing detector design and acquisition protocols, and for developing and

assessing correction and reconstruction methods (Buvat and Castiglioni 2002, Ljungberg *et al* 1998, Zaidi 1999). Several Monte Carlo simulators are currently available for PET simulations (Buvat and Castiglioni 2002, Ljungberg *et al* 1998, Zaidi 1999) and new codes are under development (Jan *et al* 2004). Each code presents some advantages and limitations with respect to the others. However, because each code has been described and validated in a specific way, it is difficult to know which code is best suited to a specific application. The purpose of this paper is twofold. First, we propose a uniform description of the features of the codes dedicated to PET simulations that could help determine *a priori* whether a code is appropriate for a specific application. Second, we present some validation procedures making use of the NEMA NU2 measurements (NEMA 1994, 2001) and involving standard criteria (e.g., spatial resolution, scatter fraction, detection sensitivity) that could be performed to characterize the accuracy of a code. Tests appropriate for reporting the computational efficiency of a code are also suggested. The relevance of the proposed code description and validation procedures is illustrated by considering two codes currently available for PET simulation.

2. Method

2.1. Description of a simulator

The current codes available to simulate PET acquisitions can be described by considering four main classes of features: (1) the models used to simulate the physics involved in PET; (2) the models used to simulate a PET acquisition (in terms of activity and attenuation distributions and detector components); (3) the acceleration strategies which determine the efficiency of the code; (4) the technical characteristics of the code which determine its portability and ease of use. A code can be described by specifying precise information related to these four types of features. As the aim of the proposed description profile is to facilitate the comparison between codes, we focus on the features that can differ from one code to another.

2.1.1. Modelling the physics. The choice of the models used to simulate the physics processes involved in PET is of foremost importance to closely reproduce real-data characteristics. These models relate to the transport of the particles through the attenuating media and to the response of the imaging system. To describe these models, the following features shall be specified:

- Description of the random number generator (function name, periodicity).
- Simulation of photoelectric effect (yes/no) and associated cross-section tables.
- Simulation of Compton scattering (yes/no) and associated cross-section tables.
- Simulation of polarization effect in the case of multiple scattering (yes/no) and associated model.
- Simulation of coherent (Rayleigh) scatter (yes/no) and associated cross-section tables.
- Simulation of the emission of x-rays following a photoelectric effect (yes/no) and associated model.
- Description of the radioisotope. For instance, ‘full decay scheme’ means that the simulator can handle all particles resulting from the decay of the radioisotope.
- Simulation of the positron mean free path (yes/no) and associated model.
- Simulation of the coincidence photon acollinearity (yes/no) and associated model.
- Simulation of the positron transport (yes/no) and associated model.
- Simulation of the photon transport in the crystal (yes/no) and associated model.
- Simulation of the electron transport in the crystal (yes/no) and associated model.
- Simulation of the scintillation photons (yes/no) and associated model.

- Simulation of the crystal radioactivity (yes/no) and associated model.
- Simulation of the detector dead time (yes/no) and associated model.
- Simulation of the pile-up phenomenon (yes/no) and associated model.
- Simulation of the finite energy resolution (yes/no) and associated model.
- Availability of energy cut-off (yes/no) making it possible to stop the tracking of particles whose energy gets below a certain threshold value.
- Simulation of the finite time resolution (yes/no) and associated model.
- Simulation of the coincidence window length (yes/no).
- Simulation of signal processing in a backcompartment (yes/no), i.e. all what is behind the crystal, especially the photomultiplier tubes and associated electronics, and associated model.
- Simulation of random coincidences (yes/no) and associated model.
- Availability of normalization correction (yes/no), to account for sensitivity variations between lines of response due to the geometry of the scanner, and corresponding normalization.
- Simulation of the arc effect (yes/no), resulting from the mapping of a curved detection surface onto a plane.
- Availability of arc effect correction (yes/no).

For all features for which an associated model should be indicated, a bibliographic reference should be given if available.

2.1.2. Modelling a PET acquisition. The relevance of simulated data will depend on the range of objects, detectors and acquisition protocols that can be simulated. To describe the type of acquisitions that can be simulated, the following information shall be given:

- Description of the activity distribution. The activity distribution can usually be described either ‘analytically’, i.e. using combination of geometric shapes or of analytical functions describing shapes, or using ‘segmented voxelized activity map’, i.e. a volume of images in which pixel values are labels, or using ‘unsegmented voxelized activity map’, i.e. a volume of images in which pixel values are proportional to activity concentration.
- Description of the attenuation distribution. The options are the same as for the description of activity distribution.
- Simulation of dynamic activity distributions (yes/no) and associated method.
- Simulation of transmission acquisitions (yes/no) and type of transmission source that can be simulated if any.
- Simulation of 2D acquisition mode (yes/no).
- Simulation of 3D acquisition mode (yes/no).
- Simulation of interplane septa (yes/no) and associated model. Any restriction should be indicated.
- Simulation of external shielding (yes/no) and associated model. Any restriction should be indicated.
- Description of the detector medium (e.g., scintillator, solid state).
- Description of the detector unit (e.g., large continuous detector, small detector: block/pixellated detectors).
- Description of scanner shape (e.g., polygonal, ring).
- Simulation of scanner motion (yes/no) and types of motion that can be simulated.

2.1.3. Acceleration strategies. The usefulness of a code strongly depends on its efficiency, i.e. on its ability to generate many coincidences in a short time. This efficiency depends on the way each particle is tracked, on whether importance sampling (Haynor 1998) is used, and also on the parallelization facilities of the codes that make it possible to follow several particles simultaneously (Zaidi *et al* 1998). To characterize the efficiency of a code, the following features shall be described:

- Use of geometric approximations (yes/no) and nature of these approximations if available.
- Use of variance reduction techniques (yes/no) and type of variance reduction techniques, if available.
- Use of parallelization facilities (yes/no) and parallelization mechanism, if available.

2.1.4. Technical characteristics. Some technical characteristics might affect the ease of implementation and of use of the code, and hence are useful to mention:

- Description of language in which the code is written.
- Description of platforms and operating systems supporting the code.
- Description of memory requirements (Mbytes) to run the code (and not to install it).
- Description of user interface (text/graphic): unlike a graphic interface, a text interface makes it possible to run simulations in a batch mode.
- Access to the code sources (yes/no).
- Debugging capability (yes/no).
- Description of the type of output information. This includes whether energy information can be output and at which level (radioactive source, single crystal, block, whole imaging system), whether time associated with different kinds of events (positron emission, positron interaction, coincident gamma emission, gamma interaction) can be recorded, and which spatial coordinates are stored (positron emission location, positron interaction location, gamma emission location, gamma interaction location).
- Description of the type of events for which information can be stored (singles, coincident events, trues, scatter, randoms and multiples).
- Description of the output data type (sinograms, list, images, energy spectra).
- Description of output files format (binary, ascii, DICOM, manufacturer format).
- Availability of the code (yes/no).
- Availability of technical documentation associated with the code (yes/no).
- Availability of technical support regarding the use of the code (yes/no).
- Availability of user group (yes/no).
- Availability of test data which can be used to test that the code runs properly (yes/no).

2.2. Validation of a simulator

Meaningful use of Monte Carlo simulated data requires a preliminary validation of the code, at least regarding features that are of interest for the problem to be addressed through simulations. For instance, using simulated data to assess scatter correction methods requires a preliminary validation of the magnitude and spatial/energy distribution of the scatter coincidences.

We propose a set of validation tests to characterize the accuracy of a code. Because the accuracy of a code is determined by its ability to generate data identical to those that would be acquired on real imaging systems, most tests involve the comparison of simulated and experimental data, using some of the NEMA NU2 1994 and 2001 phantoms (NEMA 1994, 2001), as this material is widely available. The tests relate to: (a) physical parameters characterizing the global response of a PET scanner (intrinsic spatial resolution,

scatter fraction, detection sensitivity, count rate performance), (b) spatial distributions for homogeneous and heterogeneous radioactive sources, allowing for the assessment of the local response of a PET scanner, and (c) statistical properties of the simulated data. All tests apply to the detected coincidences as sinograms, to avoid any confounding factors due to different implementations of tomographic reconstruction. Both experimental and simulated sinograms corresponding to each transaxial plane (parallel to the detector rings) shall be extracted from the 2D or 3D data using single slice rebinning.

2.2.1. Global analysis

2.2.1.1. Intrinsic spatial resolution. The intrinsic spatial resolution measurements use part of the NEMA NU2 2001 point source set up.

Data collection procedure. An ^{18}F point source with an inner diameter (ID) of 1 mm or less, an outer diameter (OD) of 2 mm or less and an axial extent less than 1 mm shall be placed in the imaging plane at the centre of the axial field of view (FOV) at two positions: (1) 1 cm vertically from the centre ($x = 0, y = 1$ cm); (2) 10 cm vertically from the centre ($x = 0, y = 10$ cm) (NEMA 2001). At least 100 kcounts shall be obtained (by experimental measurement or simulation) for each location. Real data shall be acquired with an activity concentration such that the randoms coincidence rate and count rate losses do not exceed 5% of the total coincidence rate. Random coincidences shall not be simulated.

Calculations and analysis. For each projection angle within each rebinned sinogram (i.e., each row), the location of the centre of the point source shall be determined by finding the pixel with the highest value. Each sinogram row shall then be shifted so that the pixel with the highest value is aligned with the central pixel of the sinogram. After alignment, all rows of the sinogram shall be summed to yield a single count profile per transaxial plane. To estimate the spatial resolution in transaxial planes, only the count profile corresponding to the central transaxial plane shall be considered. To estimate the axial spatial resolution, the data corresponding to the 1 cm off-centred source shall be considered: the maximum count value of each transaxial count profile shall be plotted as a function of the transaxial plane number, to yield an axial count profile. A spatial sampling of 2 mm in the three directions is recommended.

Reporting. The full width at half maximum (FWHM) and at tenth maximum (FWTM) calculated on the count profile corresponding to the central transaxial slice shall be reported for both the acquired and the simulated data, for the two positions of the point source (1 and 10 cm off-centred). The FWHM and the FWTM of the axial profile shall be reported to characterize the axial spatial resolution. This will yield a total of 6 spatial resolution values expressed in millimetres.

2.2.1.2. Scatter fraction. The scatter fraction measurements shall be performed according to the NEMA NU2 2001 guidelines.

Data collection procedure. A 700 mm ^{18}F line source, with an ID of 3.2 mm at most and an OD of 4.8 mm at most, shall be placed within a 700 mm long water cylinder, 200 mm in diameter, parallel to the tomograph axis, at a radial distance of 45 mm. The cylinder including the source shall be placed parallel to the tomograph axis. At least 500 kcounts (scatter + trues) shall be obtained in the acquired or simulated data. Experimental data shall be acquired with a randoms rate and count rate losses below 1% of the trues rate. Random coincidences shall

not be simulated. Experimental and simulated data shall not be corrected for attenuation and scatter.

Calculations and analysis. For scanners with an axial FOV longer than 65 cm, only those slices within the 65 cm central part of the axial FOV shall be considered. For tomographs with an axial FOV of 65 cm or less, all slices shall be considered. For each projection angle (i.e., each row) of each rebinned sinogram, the location of the centre of the line source shall be determined by finding the pixel with the highest value. All pixels located farther than 12 cm from that pixel shall be set to zero. Each row shall then be shifted so that the pixel containing the highest value is aligned with the central pixel of the sinogram. After alignment, the sum of the rows shall be calculated to yield a single count profile per transaxial slice. The resulting sinogram profiles shall be used to calculate the number of scatter coincidences. This number is given by the number of coincidences outside a 4 cm wide strip at the centre of the sinogram plus the number of scatter coincidences within the 4 cm region of interest (ROI). This latter number is estimated by linear interpolation between the two pixel values at the edge of the ROI (2 cm on the left and on the right of the profile centre). The number of total coincidences is given by the total number of coincidences within the 24 cm wide strip at the centre of the sinogram. For each slice, the scatter fraction is given by the number of scatter coincidences divided by the number of total coincidences. A spatial sampling of 2 mm in the three directions is recommended.

Reporting. The system scatter fraction corresponding to the average scatter fractions over all slices encompassing the 65 cm central axial FOV shall be reported (1 percentage value).

2.2.1.3. System sensitivity. The experimental tools required for performing the sensitivity measurements as recommended by the NEMA NU2 2001 procedure are not easily available yet. For this reason, the sensitivity measurement procedure as described in the NEMA NU2 1994 standards was considered. Furthermore, data collected for this procedure will be used for count rate characterization.

Data collection procedure. The 19 cm long, 20 cm in diameter cylindrical NEMA phantom filled with ^{18}F shall be centred within the tomograph field of view. At least 20 kcounts per transaxial plane shall be obtained in the experimental or simulated data. Experimental data shall be acquired with a randoms rate below 5% of the true rate. Randoms and dead time effects shall be simulated if possible, as these simulations will also be used for count rate characterization. Experimental and simulated data shall be corrected for random coincidences and dead time losses but not for attenuation. To calculate total system sensitivity, both experimental and simulated data shall not be corrected for scatter. To calculate true system sensitivity, experimental data shall be corrected for scatter and scatter shall be excluded from the simulated data.

Calculations and analysis. For each rebinned sinogram corresponding to a transaxial slice, the total number of counts within a 24 cm wide strip centred on the centre of the sinogram shall be calculated. For experimental data, the sensitivity per slice shall be calculated by dividing the total number of counts within the 24 cm region by the acquisition time and the activity concentration in the phantom. For simulated data, the sensitivity per slice shall be calculated in a similar way, as the ratio between the total collected counts in the 24 cm region and the number of simulated positrons per unit of volume in the phantom. The F18 branching ratio should be accounted for to establish the relationship between simulated positrons per unit of volume and F18 concentration. Sensitivity per slice shall be expressed in $(\text{counts s}^{-1})/(\text{Bq ml}^{-1})$. For both experimental and simulated data, the system sensitivity shall be calculated

as the sum of sensitivity per slice over all slices of the tomograph within the central 17 cm or the axial FOV whichever is less.

Reporting. For both experimental and simulated data, the total and true axial sensitivity profiles shall be plotted by reporting the estimated sensitivity per slice values against the slice number. The total and true system sensitivities shall also be reported. Thus in total, two profiles and two sensitivity values in $(\text{counts s}^{-1})/(\text{Bq ml}^{-1})$ shall be reported.

2.2.1.4. Count rate

Data collection procedure. The same set up as that used for the sensitivity measurements shall be used (cf section 2.2.1.3). Using this set up, experiments and simulations shall be performed for different activity concentrations in the phantom from 0.75 kBq ml^{-1} up to 7.5 kBq ml^{-1} . For the experimental data, the true, scatter and random coincidences shall be obtained as recommended by the manufacturer. No correction for attenuation and dead time losses shall be applied. In the simulations, true, scatter and random coincidences shall be considered. Dead time model shall be applied to simulated data if available.

Calculations and analysis. All rebinned sinograms corresponding to slices included in the central 17 cm of the axial FOV or in the whole axial FOV whichever is less shall be summed. Only the 24 cm central part of that sinogram shall be considered.

Reporting. Plots of the trues, randoms and noise-equivalent-count (NEC) rates (all in counts per second) (Strother *et al* 1990) shall be plotted as a function of the activity concentration (kBq ml^{-1}) in the phantom, yielding three plots.

2.2.2. Local analysis

2.2.2.1. *Transaxial activity profile through a homogeneous activity distribution.* A transaxial activity profile through a simple object shall be displayed to assess the match between the spatial distribution of the simulated and of the experimental coincidences.

Data collection procedure. The same set up as that used for the sensitivity measurement shall be considered (cf section 2.2.1.3).

Calculations and analysis. For each rebinned sinogram, all rows shall be added together to yield a single profile per transaxial plane. The resulting activity profiles shall then be summed axially over all slices, to yield a single activity profile corresponding to an averaging over all angles and axial slices. A spatial sampling of approximately 2 mm in the three directions is recommended.

Reporting. The transaxial activity profile (counts as a function of distance from the FOV centre) from the simulated data shall be overlapped with that from the experimental data. The two profiles shall be normalized to the same area under the curve, to emphasize the differences in spatial distribution of the counts while disregarding the differences in sensitivity.

2.2.2.2. *Transaxial activity profile through an off-centred line source embedded in a 70 cm long water cylinder.* To test the accuracy of the code in reproducing an asymmetric scatter distribution in the presence of out-of-the field of view activity, we considered a transaxial activity profile through an 8 cm off-centred line source embedded in a cylinder whose length exceeded the axial field of view (NEMA 2001 phantom for the scatter fraction measurement).

Data collection procedure. A 700 mm ^{18}F line source, with an ID of 3.2 mm at most and an OD of 4.8 mm at most, shall be placed within a 700 mm long water cylinder, 200 mm in diameter,

parallel to the tomograph axis, at a radial distance of 80 mm. The cylinder including the source shall be placed parallel to the tomograph axis and should be centred axially and transaxially. At least 500 kcounts (scatter + trues) shall be obtained in the acquired or simulated data. Experimental data shall be acquired with a randoms rate and count losses rate below 1% of the trues rate. Random coincidences shall not be simulated. Experimental and simulated data shall not be corrected for attenuation and scatter.

Calculations and analysis. For scanners with an axial FOV longer than 65 cm, only those slices within the 65 cm central part of the axial FOV shall be considered. For tomographs with an axial FOV of 65 cm or less, all slices shall be considered. The rebinned sinograms shall be summed axially to yield a single sinogram corresponding to an averaging over all axial slices. For each projection angle (i.e., each row) of the resulting sinogram, the location of the centre of the line source shall be determined by finding the pixel with the highest value. Each row shall be shifted so that the pixel containing the highest value is aligned with the central pixel of the sinogram. After alignment, the sum of the rows covering 0–90° and 90–180° shall be calculated to yield two count profiles. A spatial sampling of approximately 2 mm in the three directions is recommended.

Reporting. The asymmetric experimental and simulated profiles shall be overlapped using a semi-logarithmic representation.

2.2.2.3. Recovery of a heterogeneous-voxelized activity distribution. To complete the validation of a code, we propose a test regarding the recovery of an image from the simulated sinograms of a voxelized complex activity distribution, which does not present any specific symmetry.

Data collection procedure. The Zubal numerical phantom shall be considered (Zubal *et al* 1994). A 128 × 128 slice (4 mm × 4 mm sampling) through the thorax, including three different activity levels has been defined together with the corresponding attenuation map, involving three different attenuation media. These two activity and attenuation slices can be downloaded from <http://www.guillemet.org/mc>. Both slices shall be replicated 15 times in the axial direction to yield a 15 cm long activity volume (1 cm axial sampling). A hundred million counts shall be generated. True and scatter coincidences shall be considered.

Calculations and analysis. For the true and scatter data sets, all rebinned sinograms shall be summed together over the 15 cm corresponding to the activity volume axial extent to yield a single sinogram per data set. This single sinogram shall be corrected for attenuation using the original attenuation map and reconstructed using 2D filtered backprojection with a Ramp filter (cut-off frequency = 0.5 pixel⁻¹). A bidimensional Gaussian filter with a FWHM of 4 mm shall be applied to the reconstructed images. One-pixel (4 mm) thick central horizontal and vertical profiles shall be drawn from the reconstructed images.

Reporting. The original activity map shall be displayed together with the reconstructed trues and trues + scatter activity maps. The profiles corresponding to the reconstructed images shall be shown.

2.2.3. Statistical properties of the data. Because some reconstruction procedures assume that the acquired data follow a specific statistical distribution, it is important to verify if simulations preserve the statistical properties of the data.

Data collection procedure. The same set up as that used for sensitivity measurements shall be used (cf section 2.2.1.3). However, 20 equivalent simulations of this set up shall be performed,

keeping all parameters unchanged except the seed of the random generator. Similarly, 20 replicated experiments shall be obtained. For both experimental and simulated data, at least 10 kcounts per transaxial plane shall be collected.

Calculations and analysis. For each pixel of the rebinned sinograms, the averaged value over the 20 replicates and the associated standard deviation shall be calculated.

Reporting. A plot of the standard deviation values as a function of the averaged value shall be reported, including a number of points equal to the number of pixels in all sinograms. The function ‘standard deviation = mean^{1/2}’ shall be plotted as a reference (Yu and Fessler 2002).

2.3. Computational efficiency of the simulation code

The computational efficiency of the code can be characterized by the CPU time needed to track a coincidence event and to store the output information. Because it can differ depending on whether the object is described analytically or using a voxelized activity map (Peter *et al* 2000), it has to be measured in these two configurations. Also, because the computational time needed for a simulation highly depends on the computer system performance, it has to be normalized in some way by a number characterizing the computer performance. We propose to consider a metric provided by the Standard Performance Evaluation Corporation (SPEC) (<http://www.spec.org>).

Data collection procedure. The same set up as that used for the sensitivity measurement shall be considered (section 2.2.1.3). When activity map can be described analytically, such description shall be used for this test. To characterize the computational efficiency of the code for a voxelized source distribution—when available—the set up corresponding to the complex activity distribution recovery shall be used (section 2.2.2.3).

Calculations and analysis. For each set up (uniform short cylinder and Zubal phantom), the CPU computing time for the total simulation shall be divided by the number of generated coincidences and by the SPECfp_rate_base2000 dimensionless metric characterizing the computer used for the simulation. The values of the SPECfp_rate_base2000 metric for most computer systems are available at <http://www.spec.org>. The values of SPECfp_rate_base95 from the same Web site can be used otherwise.

Reporting. The number of generated coincidences per second normalized to the computer performance shall be reported for each set up, yielding two values.

3. Results

As a result of the proposed standardized description of a simulator, a ‘description table’ was created to list the features associated with the four main classes characterizing a simulator. For each feature, the description table includes an empty field allowing for an answer different from the given choice. Empty fields are also provided to elaborate on some features and give references to articles including details about the corresponding feature. Similarly, a ‘validation table’ was created to report the parameters and plots allowing a direct comparison between experimental and simulated data. Empty forms corresponding to these tables can be downloaded from <http://www.guillemet.org/mc>. Guidelines to fill the tables are also available on the site.

To illustrate the relevance of the suggested description profile and validation procedures, two simulators currently available for PET simulations were considered: SimSET, developed at the University of Washington (Harrison *et al* 1993, SIMSET 2001), and PET-EGS

(Castiglioni *et al* 1999), developed at the H S Raffaele PET Centre in Milano. The original SimSET v2.6.2.3 was slightly modified so that it did not use the depth of interaction information (which is not available using conventional real PET scanners) to determine the line of response. SimSET was tested without and with importance sampling (stratification, forced detection, forced non-absorption). The numbers of photon pairs simulated for calculating the different figures of merit were: 6 million pairs for each spatial resolution test, 360 million pairs for the scatter fraction estimates, 200 million pairs for the sensitivity test (also used for the activity profile calculation, the count rate estimates and the CPU performance characterization), 100 million pairs for the off-centred line source embedded in the 70 cm long water cylinder, 200 million pairs in total (i.e., about 10 million pairs per dataset) for characterizing the statistical properties of the data, and 200 million pairs for the Zubal phantom.

3.1. Description of the simulators

Table 1 summarizes the characteristics of SimSET and PET-EGS following the proposed description profile, according to the description table. References to a more complete description of the simulators are given, when available.

3.2. Validation of the simulators

The accuracy of SimSET and PET-EGS was studied by considering experiments performed on the CPET scanner (ADAC/UGM, Philadelphia, PA) and corresponding simulations. Normalization, arc correction and plane efficiency correction were not applied to data simulated by PET-EGS and SimSET and to the experimental data. The results of the validation procedures are summarized in figure 1 for SimSET without the use of importance sampling and PET-EGS, together with the experimental values measured by CPET. With SimSET, the results concerning spatial resolution, scatter fractions, sensitivity and normalized activity profiles were undistinguishable had importance sampling been used or not. As expected, importance sampling affected the statistical properties of the data (figure 1). When using importance sampling, the sinograms of the weights, which are assigned to each simulated photon history and correspond to the number of 'real world' histories that particular history represents, have to be considered (Haynor *et al* 1991). These sinograms are unbiased, as demonstrated, in our results, by the fact that all figures of merit were identical had the importance sampling techniques been turned on or not. The variance of the weights is roughly equal to the sum of the squared weights, and can also be expressed using the quality factor associated with the simulation (Haynor *et al* 1991). The curve corresponding to the theoretical standard deviation is shown as a solid line in figure 1 ($\text{std} = 14.9 \sqrt{\text{mean}}$): the estimate of the standard deviations from the 20 replicates of the simulation was in agreement with the theoretical prediction (figure 1). Although importance sampling substantially increases the computational efficiency of the code (cf section 3.3), resulting data cannot be used if the statistical properties of the simulated data are of interest. The only way to reproduce the appropriate statistical properties of simulated data while still using importance sampling is to run a long simulation to get almost noise-free data, scale it to the desired number of coincidences, and then add noise.

3.3. Computational efficiency of the code

Because the SPECfp_rate_base2000 metric was not available for the computers used to run our simulations, we considered the SPECfp_rate_base95 metric instead. The SimSET simulations were run on a Sun Ultra Sparc 10 workstation (SPECfp_rate_base95 value = 151).

Table 1. Description table filled for SimSET and PET-EGS.

		SimSET		PET-EGS	
Modelling the physics	Random number generator	Function:Random	Periodicity: 16(2e31-1)	Function:Rndm2	Periodicity: 4.6.10e18 (CERN library entry V107)
	Photoelectric effect	<input type="checkbox"/> No <input checked="" type="checkbox"/> Yes: EPDL94 (EPDL94)	<input type="checkbox"/>	<input type="checkbox"/> No <input checked="" type="checkbox"/> Yes: PHOTX (Sakamoto 1993)	<input type="checkbox"/>
	Compton scatter	<input type="checkbox"/> No <input checked="" type="checkbox"/> Yes: EPDL94 (EPDL94)	<input type="checkbox"/>	<input type="checkbox"/> No <input checked="" type="checkbox"/> Yes: PHOTX (Sakamoto 1993)	<input type="checkbox"/>
	Polarization effect	<input type="checkbox"/> No <input checked="" type="checkbox"/> Yes:	<input type="checkbox"/>	<input type="checkbox"/> No <input checked="" type="checkbox"/> Yes: PHOTX (Sakamoto 1993)	<input type="checkbox"/>
	Rayleigh scatter	<input type="checkbox"/> No <input checked="" type="checkbox"/> Yes: EPDL94 (EPDL94)	<input type="checkbox"/>	<input type="checkbox"/> No <input checked="" type="checkbox"/> Yes:	<input type="checkbox"/>
	X-rays	<input type="checkbox"/> No <input checked="" type="checkbox"/> Yes:	<input type="checkbox"/>	<input type="checkbox"/> No <input checked="" type="checkbox"/> Yes:	<input type="checkbox"/>
	Radioisotope model	<input type="checkbox"/> Full-decay <input checked="" type="checkbox"/> Positron emitter	<input type="checkbox"/> 2 511keV gamma emitter	<input type="checkbox"/> Full-decay <input checked="" type="checkbox"/> Positron emitter	<input type="checkbox"/> 2 511keV gamma emitter
	Positron mean-free path	<input type="checkbox"/> No <input checked="" type="checkbox"/> Yes: Analytical	<input checked="" type="checkbox"/> Monte Carlo	<input type="checkbox"/> No <input checked="" type="checkbox"/> Yes: Analytical	<input checked="" type="checkbox"/> Monte Carlo
	Photon acollinearity	<input type="checkbox"/> No <input checked="" type="checkbox"/> Yes: Analytical	<input checked="" type="checkbox"/> Monte Carlo	<input type="checkbox"/> No <input checked="" type="checkbox"/> Yes: Analytical	<input checked="" type="checkbox"/> Monte Carlo
	Positron transport	<input type="checkbox"/> No <input checked="" type="checkbox"/> Yes: Analytical	<input checked="" type="checkbox"/> Monte Carlo	<input type="checkbox"/> No <input checked="" type="checkbox"/> Yes: Analytical	<input checked="" type="checkbox"/> Monte Carlo
	Photon transport in crystal	<input type="checkbox"/> No <input checked="" type="checkbox"/> Yes: Analytical	<input checked="" type="checkbox"/> Monte Carlo	<input type="checkbox"/> No <input checked="" type="checkbox"/> Yes: Analytical	<input checked="" type="checkbox"/> Monte Carlo
	Electron transport	<input type="checkbox"/> No <input checked="" type="checkbox"/> Yes: Analytical	<input checked="" type="checkbox"/> Monte Carlo	<input type="checkbox"/> No <input checked="" type="checkbox"/> Yes: Analytical	<input checked="" type="checkbox"/> Monte Carlo
	Scintillation photons	<input type="checkbox"/> No <input checked="" type="checkbox"/> Yes: Analytical	<input checked="" type="checkbox"/> Monte Carlo	<input type="checkbox"/> No <input checked="" type="checkbox"/> Yes: Analytical	<input checked="" type="checkbox"/> Monte Carlo
	Crystal radioactivity	<input type="checkbox"/> No <input checked="" type="checkbox"/> Yes: Analytical	<input checked="" type="checkbox"/> Monte Carlo	<input type="checkbox"/> No <input checked="" type="checkbox"/> Yes: Analytical	<input checked="" type="checkbox"/> Monte Carlo
	Detector dead time	<input type="checkbox"/> No <input checked="" type="checkbox"/> Yes: Analytical	<input checked="" type="checkbox"/> Monte Carlo	<input type="checkbox"/> No <input checked="" type="checkbox"/> Yes: Analytical	<input checked="" type="checkbox"/> Monte Carlo
	Pile-up model	<input type="checkbox"/> No <input checked="" type="checkbox"/> Yes:	<input type="checkbox"/>	<input type="checkbox"/> No <input checked="" type="checkbox"/> Yes:	<input type="checkbox"/>
	Finite energy resolution	<input type="checkbox"/> No <input checked="" type="checkbox"/> Yes: Analytical	<input checked="" type="checkbox"/> Monte Carlo	<input type="checkbox"/> No <input checked="" type="checkbox"/> Yes: Analytical	<input checked="" type="checkbox"/> Monte Carlo
	Energy cut-off	<input type="checkbox"/> No <input checked="" type="checkbox"/> Yes: no tracking when photon energy < a user-specified threshold	<input type="checkbox"/>	<input type="checkbox"/> No <input checked="" type="checkbox"/> Yes: no tracking when photon energy < a user-specified threshold	<input type="checkbox"/>
Finite time resolution	<input type="checkbox"/> No <input checked="" type="checkbox"/> Yes: Analytical	<input checked="" type="checkbox"/> Monte Carlo	<input type="checkbox"/> No <input checked="" type="checkbox"/> Yes: Analytical	<input checked="" type="checkbox"/> Monte Carlo	
Coincidence window	<input type="checkbox"/> No <input checked="" type="checkbox"/> Yes:	<input type="checkbox"/>	<input type="checkbox"/> No <input checked="" type="checkbox"/> Yes:	<input type="checkbox"/>	
Backcompartment model	<input type="checkbox"/> No <input checked="" type="checkbox"/> Yes: juxtaposition of empirical layers	<input type="checkbox"/>	<input type="checkbox"/> No <input checked="" type="checkbox"/> Yes: analytical model (Castiglioni et al. 2002)	<input type="checkbox"/>	
Random events model	<input type="checkbox"/> No <input checked="" type="checkbox"/> Yes:	<input type="checkbox"/>	<input type="checkbox"/> No <input checked="" type="checkbox"/> Yes: Monte Carlo model (Castiglioni et al. 2002)	<input type="checkbox"/>	
Normalization	<input type="checkbox"/> No <input checked="" type="checkbox"/> Yes:	<input type="checkbox"/>	<input type="checkbox"/> No <input checked="" type="checkbox"/> Yes:	<input type="checkbox"/>	
Arc effect	<input type="checkbox"/> No <input checked="" type="checkbox"/> Yes:	<input type="checkbox"/>	<input type="checkbox"/> No <input checked="" type="checkbox"/> Yes:	<input type="checkbox"/>	
Arc correction	<input type="checkbox"/> No <input checked="" type="checkbox"/> Yes:	<input checked="" type="checkbox"/> introduced in our SimSET version	<input type="checkbox"/> No <input checked="" type="checkbox"/> Yes:	<input type="checkbox"/>	
Modelling a PET acquisition	Activity distribution	<input checked="" type="checkbox"/> Analytical	<input checked="" type="checkbox"/> Segmented voxel-based: 256 levels	<input checked="" type="checkbox"/> Analytical	<input checked="" type="checkbox"/> Segmented voxel-based: 32768 levels
	Attenuation distribution	<input type="checkbox"/> Unsegmented voxel-based	<input checked="" type="checkbox"/> Analytical and voxel-based	<input type="checkbox"/> Unsegmented voxel-based	<input checked="" type="checkbox"/> Analytical and voxel-based
	Dynamic distributions	<input checked="" type="checkbox"/> Analytical	<input checked="" type="checkbox"/> Segmented voxel-based: 256 levels	<input checked="" type="checkbox"/> Analytical	<input checked="" type="checkbox"/> Segmented voxel-based: 32768 levels
	Transmission acquisitions	<input type="checkbox"/> Unsegmented voxel-based	<input checked="" type="checkbox"/> Analytical and voxel-based	<input type="checkbox"/> Unsegmented voxel-based	<input checked="" type="checkbox"/> Analytical and voxel-based
	2D acquisition mode	<input type="checkbox"/> No <input checked="" type="checkbox"/> Yes:	<input type="checkbox"/>	<input type="checkbox"/> No <input checked="" type="checkbox"/> Yes:	<input type="checkbox"/>
	3D acquisition mode	<input type="checkbox"/> No <input checked="" type="checkbox"/> Yes: HR HS	<input type="checkbox"/>	<input type="checkbox"/> No <input checked="" type="checkbox"/> Yes: HR HS	<input type="checkbox"/>
	Interplane septa	<input type="checkbox"/> No <input checked="" type="checkbox"/> Yes: Fully HR, HS	<input type="checkbox"/> Re-binning <input type="checkbox"/> Spanning	<input type="checkbox"/> No <input checked="" type="checkbox"/> Yes: Fully HR, HS	<input type="checkbox"/> Re-binning <input checked="" type="checkbox"/> Spanning
	External shielding	<input type="checkbox"/> No <input checked="" type="checkbox"/> Yes: Any dimension	<input type="checkbox"/> Any location <input type="checkbox"/> Perfect absorber	<input type="checkbox"/> No <input checked="" type="checkbox"/> Yes: Any dimension	<input type="checkbox"/> Any location <input type="checkbox"/> Perfect absorber
	Detector medium	<input type="checkbox"/> No <input checked="" type="checkbox"/> Yes: Analytical	<input checked="" type="checkbox"/> Monte Carlo	<input type="checkbox"/> No <input checked="" type="checkbox"/> Yes: Analytical	<input checked="" type="checkbox"/> Monte Carlo
	Detector unit	<input checked="" type="checkbox"/> Scintillator <input type="checkbox"/> Solid state	<input type="checkbox"/> Any dimension <input type="checkbox"/> Any location	<input checked="" type="checkbox"/> Scintillator <input type="checkbox"/> Solid state	<input type="checkbox"/> Any dimension <input type="checkbox"/> Any location
	Scanner shape	<input checked="" type="checkbox"/> Large detector <input type="checkbox"/> Small detector: Block Pixellated Any.size	<input type="checkbox"/>	<input checked="" type="checkbox"/> Large detector <input type="checkbox"/> Small detector: Block Pixellated Any.size	<input type="checkbox"/>
	Scanner motion	<input type="checkbox"/> Polygonal <input checked="" type="checkbox"/> Ring	<input type="checkbox"/> Rotating <input type="checkbox"/> Translating <input type="checkbox"/> Wobbling	<input type="checkbox"/> Polygonal <input checked="" type="checkbox"/> Ring	<input type="checkbox"/> Rotating <input type="checkbox"/> Translating <input type="checkbox"/> Wobbling
Acceleration strategies	Geometric approximations	<input type="checkbox"/> No <input checked="" type="checkbox"/> Yes: Acceptance angle	<input type="checkbox"/>	<input type="checkbox"/> No <input checked="" type="checkbox"/> Yes: Forced detection Stratification	<input type="checkbox"/>
	Variance reduction techniques	<input type="checkbox"/> No <input checked="" type="checkbox"/> Yes: Forced detection Stratification	<input checked="" type="checkbox"/> Forced non-absorption	<input type="checkbox"/> No <input checked="" type="checkbox"/> Yes: Forced detection Stratification	<input type="checkbox"/>
	Parallelisation facilities	<input type="checkbox"/> No <input checked="" type="checkbox"/> Yes: Parallel language	<input checked="" type="checkbox"/> Parallel runs	<input type="checkbox"/> No <input checked="" type="checkbox"/> Yes: Parallel language	<input checked="" type="checkbox"/> Parallel runs
Technical features	Language	C		Fortran, C, matlab	
	Platforms/operating systems	All platforms operating UNIX		UNIX for SUN platforms	
	Memory requirements	500 Mbytes		300 Mbytes	
	User interface	<input checked="" type="checkbox"/> Text <input type="checkbox"/> Graphics		<input checked="" type="checkbox"/> Text <input type="checkbox"/> Graphics	
	Access to the source code	<input type="checkbox"/> No <input checked="" type="checkbox"/> Yes		<input type="checkbox"/> No <input checked="" type="checkbox"/> Yes	
	Debugging capability	<input type="checkbox"/> No <input checked="" type="checkbox"/> Yes		<input type="checkbox"/> No <input checked="" type="checkbox"/> Yes	
	Output information				
	- energy spectra	<input type="checkbox"/> Single crystal <input type="checkbox"/> Block crystal <input checked="" type="checkbox"/> System <input type="checkbox"/> Source	<input type="checkbox"/> none	<input checked="" type="checkbox"/> Single crystal <input checked="" type="checkbox"/> Block crystal <input checked="" type="checkbox"/> System <input checked="" type="checkbox"/> Source	<input type="checkbox"/>
	- time	<input type="checkbox"/> β+ emission <input type="checkbox"/> β+ interaction <input type="checkbox"/> γ emission <input type="checkbox"/> γ interaction	<input type="checkbox"/>	<input type="checkbox"/> β+ emission <input type="checkbox"/> β+ interaction <input checked="" type="checkbox"/> γ emission <input checked="" type="checkbox"/> γ interaction	<input type="checkbox"/>
	- spatial coordinates	<input type="checkbox"/> β+ emission <input type="checkbox"/> β+ interaction <input type="checkbox"/> γ emission <input checked="" type="checkbox"/> γ interaction	<input type="checkbox"/>	<input type="checkbox"/> β+ emission <input type="checkbox"/> β+ interaction <input checked="" type="checkbox"/> γ emission <input checked="" type="checkbox"/> γ interaction	<input type="checkbox"/>
	- incident angle	<input type="checkbox"/> No <input type="checkbox"/> Yes	<input type="checkbox"/>	<input type="checkbox"/> No <input checked="" type="checkbox"/> Yes	<input type="checkbox"/>
	Output events	<input checked="" type="checkbox"/> Singles <input checked="" type="checkbox"/> Coincidences <input checked="" type="checkbox"/> Trues	<input type="checkbox"/>	<input checked="" type="checkbox"/> Singles <input checked="" type="checkbox"/> Coincident events <input checked="" type="checkbox"/> Trues	<input type="checkbox"/>
Output data	<input checked="" type="checkbox"/> Scatter:9th order <input type="checkbox"/> Randoms <input type="checkbox"/> Multiples: order	<input type="checkbox"/>	<input checked="" type="checkbox"/> Scatter:inft order <input checked="" type="checkbox"/> Randoms <input type="checkbox"/> Multiples: order	<input type="checkbox"/>	
Output file format	<input checked="" type="checkbox"/> Sinograms <input checked="" type="checkbox"/> List <input type="checkbox"/> Images <input checked="" type="checkbox"/> Energy spectra	<input type="checkbox"/>	<input checked="" type="checkbox"/> Sinograms <input checked="" type="checkbox"/> List <input type="checkbox"/> Images <input checked="" type="checkbox"/> Energy spectra	<input type="checkbox"/>	
Code availability	<input type="checkbox"/> Binary <input type="checkbox"/> Ascii <input type="checkbox"/> DICOM <input type="checkbox"/> Company specific	<input type="checkbox"/>	<input type="checkbox"/> Binary <input type="checkbox"/> Ascii <input type="checkbox"/> DICOM <input type="checkbox"/> Company specific	<input type="checkbox"/>	
Technical documentation	<input type="checkbox"/> No <input checked="" type="checkbox"/> Yes: Public domain <input type="checkbox"/> From authors	<input type="checkbox"/>	<input type="checkbox"/> No <input checked="" type="checkbox"/> Yes: Public domain <input checked="" type="checkbox"/> From authors	<input type="checkbox"/>	
Technical support	<input type="checkbox"/> No <input checked="" type="checkbox"/> Yes:	<input type="checkbox"/>	<input type="checkbox"/> No <input checked="" type="checkbox"/> Yes:	<input type="checkbox"/>	
User group	<input type="checkbox"/> No <input checked="" type="checkbox"/> Yes:	<input type="checkbox"/>	<input type="checkbox"/> No <input checked="" type="checkbox"/> Yes:	<input type="checkbox"/>	
Test data	<input type="checkbox"/> No <input checked="" type="checkbox"/> Yes:	<input type="checkbox"/>	<input type="checkbox"/> No <input checked="" type="checkbox"/> Yes: http://www.ibfm.cnr.it/mcpet/index.html	<input type="checkbox"/>	

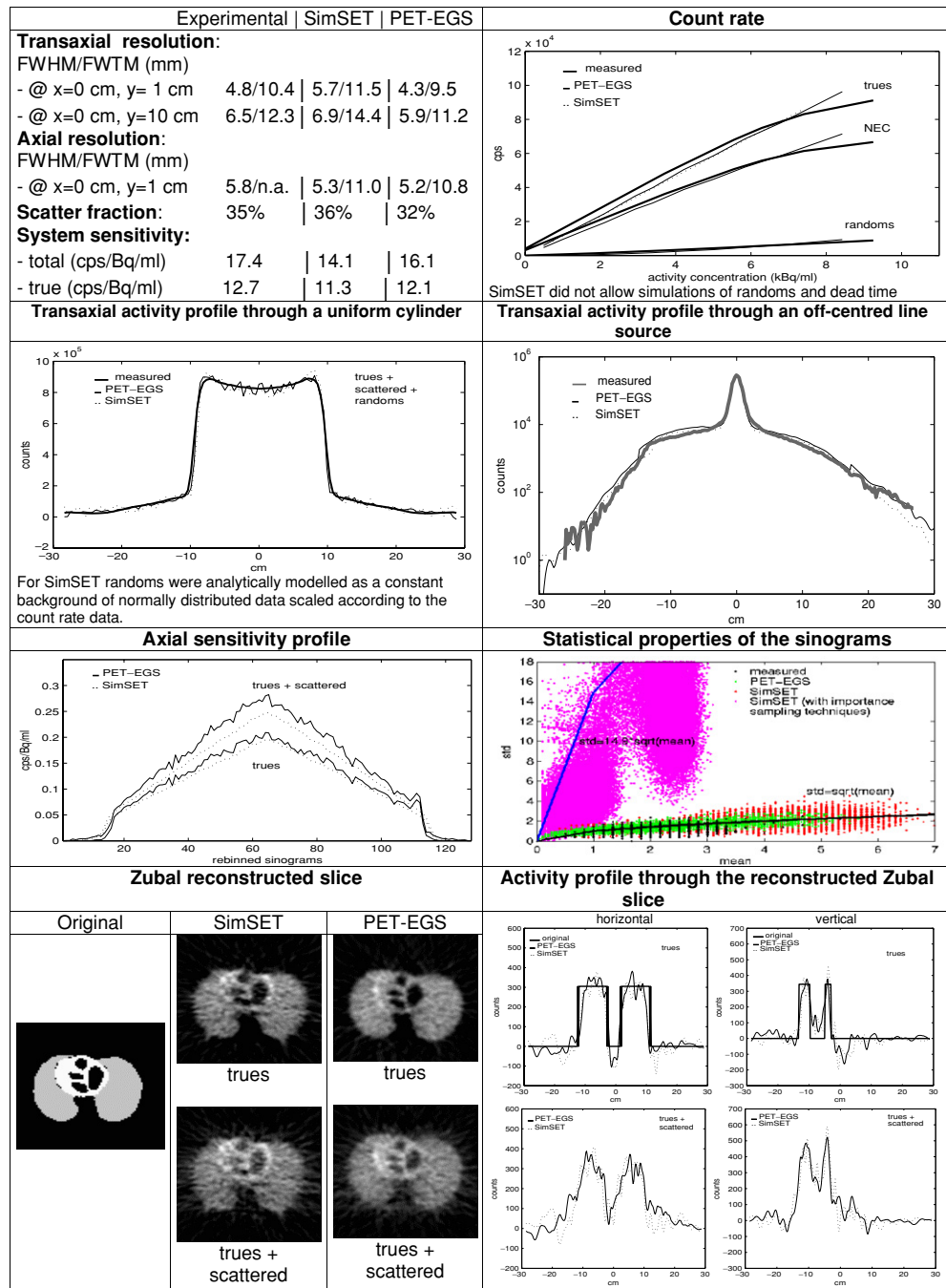


Figure 1. Summary of the validation results for SimSET and PET-EGS. All SimSET results correspond to those obtained without variance reduction techniques, except for the statistical properties.

(This figure is in colour only in the electronic version)

The PET-EGS simulations were run on a Sun Enterprise 450 workstation (SPECfp_rate_base95 value of 392); high SPECfp_rate_base95 value corresponds to high throughput of the machine.

For the short uniform cylinder experiment, PET-EGS generated 93 coincidences per second, while SimSET without importance sampling generated 1266 coincidences per second. Normalizing to the computer performance, it thus appears that SimSET was about 35 times faster than PET-EGS for the short uniform cylinder (8.38 coincidence per second against 0.24). When turning the importance sampling on with SimSET, the number of detected coincidences per second was 1.9 greater than without importance sampling.

For the voxelized Zubal phantom, PET-EGS generated 162 coincidences per second, while SimSET generated 2941 coincidences per second. Given the differences in computer performance, SimSET was about 47 times faster than PET-EGS for the voxelized Zubal phantom (19.48 coincidence per second against 0.41). Using importance sampling in SimSET, the number of detected coincidences per second was 5.4 greater than without importance sampling. The speedup factors resulting from the use of importance sampling with SimSET are consistent with those reported by Harrison *et al* (2002) for realistic configurations.

4. Discussion

The increasingly widespread use of Monte Carlo simulations in PET makes it relevant to have a good understanding of the specific features of the different codes available for performing Monte Carlo simulations. A precise characterization of these features would be helpful to determine which code is best suited to a specific application. In this work, we propose unified description and validation protocols of Monte Carlo simulators dedicated to PET simulations, to facilitate the analysis of different code features and performances. Differences between codes can be considered at three intricate levels: the design of the code, its accuracy and its computational efficiency. To give a comprehensive picture of each code, we propose to describe a code at these three levels according to a well-defined unified scheme.

4.1. Description of a simulator

At the design level, the features of a code can be classified into four classes.

The first class of features relates to the models used to describe the physics involved in PET (e.g., interactions between particles and matter, detector response). These models directly affect the *accuracy* of the code. Although the physics involved in PET is well known and understood, none of the features included in this class obeys a unique model. For instance, the choice of the cross-section tables that govern the probability of different interactions can make a difference in results (Zaidi 2000).

The second class of features concerns the way a real PET acquisition is modelled, including the way the phantom or patient and detector is described. This class of features determines the *flexibility* of the code in terms of configurations that might be simulated—regardless of how accurate the result will be. An important feature in this class is the way the activity and attenuation distributions can be input in the code (Peter *et al* 2000): only those codes allowing for the use of unsegmented voxel-based activity and attenuation maps can use patient images as input. Using patient images as an input of Monte Carlo simulations might be more and more useful in future, for instance for patient-driven scatter correction (Levin *et al* 1995, Watson *et al* 1997) or for generating highly realistic PET data sets. The type of detectors that can be modelled and the details with which the detector components can be described also strongly determine the applicability of the code to investigate new detector designs.

A third class of features relates to the acceleration techniques available to improve the throughput of the code. These features determine the *computational efficiency* of the code. The use of acceleration techniques might affect the response of the code and the output of the code might be different, depending on whether the acceleration techniques are turned on or off (Haynor 1998). In addition to specifying these features when describing a code, the acceleration techniques used for the validation tests should therefore be clearly specified.

The fourth class of features concerns technical characteristics of the code that might be of paramount importance to determine whether a code can be used in the context it has to. These features fully determine the *practical applicability* of the code in a specific environment. For instance, the portability of a code increases its possible diffusion, lack of documentation prevents from a widespread distribution, while the existence of user groups and continuous technical support facilitates its use.

This analysis of the features characterizing a Monte Carlo code has produced a 'description table', which can be freely downloaded. This table contents cannot fully characterize each code, and is not exhaustive by any mean, as each code has its own specific features that a summary table cannot fully describe. However, it gives a synthetic description of a code that should be useful for a first overview of the code capabilities and for pinpointing the major differences between codes. To demonstrate the feasibility and the relevance of this unified description, the table was filled for SimSET and PET-EGS (table 1). The description of the two codes was possible, even for SimSET that was not developed by us. Differences between the two codes were shown in the four classes of features and can be synthesized as follows: (1) SimSET is more accurate in physics modelling, although randoms and deadtime are not simulated; (2) PET-EGS is more flexible in modelling PET acquisitions (input activity distribution and scanner design description); (3) SimSET implements acceleration strategies that make the code run faster; (4) better portability is warranted by SimSET, but PET-EGS provides test data that are lacking for SimSET.

In summary, the description table makes it possible to standardize the description of a Monte Carlo simulator. It summarizes the potentials and limitations of each code, which may help the potential user find the code most appropriate for a specific application.

4.2. Validation of a simulator

Although the description of a Monte Carlo code presented above gives information regarding the expected accuracy of the code, accuracy tests have to be conducted to fully characterize its reliability. To this end, we propose a validation protocol based on the comparison between simulated and experimental data. This protocol is based on the NEMA NU2 standards and materials as often as possible for two reasons. First, the NEMA standards are widely accepted and associated materials are widely available. Second, NEMA NU2 values have been already published for a number of PET imaging systems, so some 'reference' values are already available for these systems and do not have to be repeated for validating the Monte Carlo simulator. We did not always exactly consider the NEMA NU2 standards however. Only some representative tests were selected, as a trade-off between completeness of the validation and time required, in consideration of the high computation burden required by Monte Carlo simulations. Furthermore, to avoid introducing confounding effects in the comparison of experimental and simulated data, data should be compared before any reconstruction procedure. We thus replaced some of the NEMA figures of merit involving reconstructed data by other indices to be calculated directly from the sinograms.

As a general criterion, the tests proposed in the most recent NEMA NU2 2001 were considered. However, as the NEMA NU2 2001 phantom required for sensitivity measurements

is not easily available yet, we used the NEMA NU2 1994 sensitivity measurements instead. However, the physical meaning of detection sensitivity defined as percentage of detected coincidences with respect to emitted positrons is closer to the absolute sensitivity measurable by the NEMA-NU2 (2001) protocol (Bailey *et al* 1991) and to a value that can be easily obtained using Monte Carlo simulations (percentage of collected coincidences with respect to generated positrons). Actually, comparing the CPET absolute sensitivity as estimated using the NEMA-NU2 (2001) protocol (3.0 % from Adam *et al* (2001)) with the percentage of collected coincidences with respect to simulated positrons (2.8% and 2.2% for SimSET and PET-EGS, respectively) suggested a good agreement between these two quantities.

In addition to the global parameters proposed by NEMA, procedures testing whether the local spatial response of the scanner is properly modelled by the simulator were included in the validation procedure. The local tests are based on the comparison of experimental and simulated spatial activity profiles and images. The simulation involving the voxelized non-homogeneous activity distribution from the Zubal phantom completes the local tests. It is the only test involving non-symmetric, voxelized and non-homogeneous activity and attenuation distributions. Although it cannot be considered as a test characterizing the accuracy of the code, the fidelity of the reconstructed image to the initial activity map can at least demonstrate that the code is properly handling complex activity and attenuation distributions.

Finally, a test regarding the statistical properties of the simulated data was proposed, as this is relevant for assessing statistical reconstruction algorithms using simulated data. As the statistical properties of the simulated data should not theoretically depend on the simulated phantom, the configuration simulated for this test actually does not matter much, as long as about 20 replicates of the same data are available.

It is possible that for some scanners, the conditions in which data should be acquired for the test cannot be achieved. For instance, for LSO scanners, the randoms rates will never fall below 5% as required by the proposed procedure, because of the intrinsic radiation from Lu176. In those cases, conditions as close to the recommended conditions as possible should be used for experimental measurements and for simulations, and these should be precisely described when reporting the 'validation table'.

Among the additional criteria that could be considered for validating a code, the energy spectra of the detected coincidences are of interest. We did not include any comparison of simulated with experimental energy spectra in our protocol because of the difficulty in recording energy spectra from real PET systems.

The validation protocol was applied to SimSET and PET-EGS (figure 1). For both codes, errors in the global analysis (spatial resolution, scatter fraction, system sensitivity and count rate) were never larger than 20%, suggesting that despite the differences in modelling the physics and the acquisition, the two codes produce data close to experimental data.

For the CPET, axial sensitivity profiles were not experimentally available but the agreement between the two simulated profiles, which presented the expected trend, suggests a consistent simulation of the scanner axial response.

Count rate curves from experiments and simulations showed a good agreement. At low (1.85 kBq ml⁻¹), medium (3.7 kBq ml⁻¹) and high (7.4 kBq ml⁻¹) count rates, the PET-EGS true count rates differed from the experimental ones by -16.8%, -8.8% and 4.6% respectively, while the SimSET true count rates differed from the experimental ones by -18%, -10.5% and 3.6% respectively. As PET-EGS includes a model of randoms and deadtime, it makes it possible to estimate the NEC curve. PET-EGS should thus be used instead of SimSET in simulation studies focussing on the count rate performance. At low, medium and high count rates, the NEC as estimated by PET-EGS differed from the experimental NEC by -14.6%, -7.4% and 4.3%, respectively.

For both codes, a good agreement between the experimental and simulated data was observed for the transaxial profiles across the uniform cylinder, although the shape of the SimSET transaxial profile appeared slightly more different from the measured data than did the shape of the PET-EGS profile. Since the CPET scanner did not allow randoms to be corrected independently from scatter, randoms had to be included for the comparison. Randoms were Monte Carlo modelled using PET-EGS (Castiglioni *et al* 2002) and analytically modelled (constant background, see figure 1) for SimSET. Regarding the transaxial profiles through the off-centred line source embedded in the 70 cm long water cylinder, the asymmetry of the experimental profile was reproduced by the two simulators, and both SimSET and PET-EGS yielded profiles in excellent agreement with the experimental profile.

Qualitative inspection of the Zubal phantom images proved the ability of the two simulators to simulate realistic patient data. The similarity of the trues + scattered profiles produced by the two codes confirmed the consistency of the simulations.

Comparing the statistical properties of the experimental and simulated data suggested that both codes could be used for assessing statistical reconstruction methods provided importance sampling was not used in SimSET. When using importance sampling, as expected, the variance of the produced data significantly departed from that predicted from the mean image by assuming a Poisson distribution of the detected counts, confirming that data simulated with importance sampling are not reliable in terms of variance, although they are in terms of mean.

4.3. Characterization of a code computational efficiency

The efficiency of a code has to be taken into account when deciding whether a code can fulfil the conditions needed for the intended application. Comparing the time needed for a simulation performed using different codes and different platforms is difficult. Some indications regarding the efficiency of a code can be provided by reporting CPU times for well-defined configurations, if the CPU time is normalized by a metric related to the computer performance. We suggested the use of the SPECfp_rate_base2000 as a normalization factor (<http://www.spec.org>). This metric is widely accepted for comparing compute-intensive performance across various computer architectures. Using this normalization approach, the normalized computer time per generated coincidence can be compared between codes.

Large differences in code efficiency were observed between SimSET with PET-EGS (section 3.3). Several factors can explain these differences. First, PET-EGS is based on the EGS4 code, which is known not to be efficient for the computation of the intersections between photon path and borders between different media. Second, PET-EGS systematically saves a comprehensive list of spatial, energy and time information relating to all detected coincidences while SimSET only saves specific features as requested by the user. Third, the geometrical model of the detector is more complex in PET-EGS than in SimSET: in PET-EGS, the CPET scanner was simulated using six curved crystals (hence lots of intersections have to be calculated for each crystal) while in SimSET, the scanner was modelled as a ring. Lastly, end shieldings of the CPET are not perfect absorbers in PET-EGS, unlike in SimSET.

5. Conclusion

We introduced a description profile and validation tests for characterizing Monte Carlo simulators of PET acquisitions. The feasibility of a unified description and of a unified reporting of the accuracy and computational efficiency of simulators was demonstrated by

considering two state-of-the-art Monte Carlo codes: SimSET and PET-EGS. Analysis of other PET simulators using the proposed description and validation procedures could help researchers choose an appropriate PET Monte Carlo simulator for the intended application.

Acknowledgments

This work was performed as part of the Galileo project number 04368WF, funded by the Integrated Action Program Egide of the French Ministry of Foreign Affairs and by the Italian Ministry of University and Scientific and Technological Research and CRUI. The authors thank Federica Fioroni for assistance in conducting some experiments on the CPET and the reviewers for insightful comments. The authors also gratefully acknowledge Robert Harrison for his patience and the time he spent explaining to us the subtleties of variance reduction techniques in SimSET.

References

- Adam L E, Karp J S, Daube-Witherspoon M E and Smith R J 2001 Performance of a whole-body PET scanner using curve-plate NaI(Tl) detectors *J. Nucl. Med.* **42** 1821–30
- Bailey D L, Jones T and Spinks T J 1991 A method for measuring the absolute sensitivity of positron emission tomographic scanners *Eur. J. Nucl. Med.* **18** 374–9
- Buvat I and Castiglioni I 2002 Monte Carlo simulations in SPET and PET *Q. J. Nucl. Med.* **46** 48–61
- Castiglioni I, Cremonesi O, Gilardi M C, Bettinardi V, Rizzo G, Savi A, Bellotti E and Fazio F 1999 Scatter correction techniques in 3D PET: a Monte Carlo evaluation *IEEE Trans. Nucl. Sci.* **46** 2053–8
- Castiglioni I, Cremonesi O, Gilardi M C, Savi A, Bettinardi V, Rizzo G, Bellotti E and Fazio F 2002 A Monte Carlo model of noise components in 3D PET *IEEE Trans. Nucl. Sci.* **49** 2297–303
- EPDL94, Lawrence Livermore National Laboratory, Livermore, CA, UCRL-ID 117 796, 1994
- Harrison R L, Dhavala S, Kumar P N, Shao Y, Manjeshwar R, Lewellen T K and Jansen F P 2002 Acceleration of SimSET photon history generator. *Conf. Rec. IEEE Nucl. Sci. Symp. and Med. Imaging Conf.* **3** 1835–8
- Harrison R L, Vannoy S D, Haynor D R, Gillipsie S B, Kaplan M S and Lewellen T K 1993 Preliminary experience with the photon history generator module of a public domain simulation system for emission tomography *Conf. Rec. IEEE Nucl. Sci. Symp. and Med. Imaging Conf.* **2** 1154–8
- Haynor D R 1998 *Variance Reduction Techniques Monte Carlo Calculations in Nuclear Medicine* ed M Ljungberg, S E Strand and M A King (Bristol: Institute of Physics Publishing) pp 13–24
- Haynor D R, Harrison R L and Lewellen T K 1991 The use of importance sampling techniques to improve the efficiency of photon tracking in emission tomography simulations *Med. Phys.* **18** 990–1001
- Jan S *et al* 2004 GATE: a simulation toolkit for PET and SPECT *Phys. Med. Biol.* **49** 4543–61
- Levin C S, Dahlbom M and Hoffman E J 1995 A Monte Carlo correction for the effect of Compton scattering in 3D PET brain imaging *IEEE Trans. Nucl. Sci.* **42** 1181–5
- Ljungberg M, Strand S E and King M A 1998 *Monte Carlo Calculations in Nuclear Medicine* ed M Ljungberg, S E Strand and M A King (Bristol: Institute of Physics Publishing)
- NEMA 1994 NEMA standards publication NU2-1994 performance measurements of positron emission tomographs (Washington, DC: National Electrical Manufacturers Association)
- NEMA 2001 NEMA standards publication NU2-2001 performance measurements of positron emission tomographs (Rosslyn, VA: National Electrical Manufacturers Association)
- Peter J, Tornai M P and Jaszczak R J 2000 Analytical versus voxelized phantom representation for Monte Carlo simulation in radiological imaging *IEEE Trans. Med. Imaging* **19** 556–64
- Sakamoto Y 1993 Photon cross section data PHOTX for PEGS4 code *Proc. 3rd EGS4 Users's Meeting (Japan)* pp 77–82
- SIMSET 2001 *SIMSET Overview* http://depts.washington.edu/~simset/html/simset_home.html
- Strother S C, Casey M E and Hoffman E J 1990 Measuring PET scanner sensitivity: relating countrates to image signal-to-noise ratios using noise equivalent counts *IEEE Trans. Nucl. Sci.* **37** 783–8
- Watson C C, Newport D, Casey M E, deKemp A, Beanlands R S and Schmand M 1997 Evaluation of simulation-based scatter correction for 3D PET cardiac imaging *IEEE Trans. Nucl. Sci.* **44** 90–7
- Yu D F and Fessler J A 2002 Mean and variance of coincidence counting with deadtime *Nucl. Instrum. Methods Phys. Res. A* **488** 362–74

-
- Zaidi H 1999 Relevance of accurate Monte Carlo modeling in nuclear medical imaging *Med. Phys.* **26** 574–608
- Zaidi H 2000 Comparative evaluation of photon cross section libraries for materials of interest in PET Monte Carlo simulations *IEEE Trans. Nucl. Sci.* **47** 2722–35
- Zaidi H, Labbe C and Morel C 1998 EIDOLON: implementation of an environment for Monte Carlo simulation of fully 3D positron tomography on a high-performance parallel platform *Parallel Comput.* **24** 1523–36
- Zubal I G, Harrell C R and Smith E 1994 Computerized 3D segmented human anatomy *Med. Phys.* **21** 299–302